scientific reports

Check for updates

OPEN

Research on seismic activity and seismic structural characteristics of the Shandong region

Linhai Lu[1], Zhenghao Liu[2,3]✉, Hanwen Zhang[2], Chaojun Wu[1], Jiecheng Sun[1], Xianfeng Ma[2]✉, Dingyi Zhou[2], Han Han[2], Haojin Zhang[2] & Rui Li[2]

This study provides a comprehensive analysis of seismic activity and structural characteristics in Shandong Province, China, with a focus on identifying seismic belts and potential epicentral zones critical for regional seismic safety. A detailed database was developed, integrating regional seismicity statistics, earthquake distribution patterns, significant geotectonic movements, and recent neotectonic activities. The results reveal that seismic activity in Shandong is heterogeneously distributed, with moderate to strong earthquakes predominantly associated with active fault zones and exhibiting zonal clustering. Earthquakes are generally shallow, occurring within the middle to upper crust, with historical destructive events averaging a focal depth of 19 km, while recent minor seismic events average 14.9 km in depth. These activities span North China Plain and Tan-Lu Seismic Statistical Areas. Projections indicate sustained or heightened seismic activity over the next century, with the potential for earthquakes up to magnitude 5. The geological framework is dominated by Luxi Fault Block and Tan-Lu Fault Zone, characterized by episodic uplift and subsidence driven by neotectonic movements. The prevailing horizontal tectonic stress regime supports the likelihood of strike-slip faulting as the predominant mechanism.

Keywords Seismic activity, Structural features, Database, Earthquake hazard assessment

Earthquake disasters pose a significant threat to many regions worldwide, necessitating comprehensive investigations into seismicity and tectonic structures to mitigate potential risks. Shandong Region (between 116° to 123° east longitude and 34° to 38° north latitude, Fig. 1), located in the southern part of the North China Plain, is affected by the combined influences of the Eurasian, Philippine Sea, and Pacific tectonic plates, rendering it prone to major earthquakes and associated hazards. A prominent seismogenic feature in this region is the Tancheng-Lujiang Fault Zone, traversing the eastern part of Shandong and ranking among the most active fault belts in Eastern China. Historical seismic events, such as the Tancheng earthquake on July 25, 1668 (M_s = 8.5, M_s refers to the surface-wave magnitude), one of the most significant recorded earthquakes in Chinese history, Caoxian earthquake on August 10, 1937 (M_s = 7.0), and the Tangshan earthquake aftershock on July 28, 1976 (M_s = 7.5), underscore the potential for devastating seismic disasters in this area[1–3].

Earthquake hazard assessment is essential for developing effective risk-mitigation strategies, guiding land-use planning, and formulating earthquake-resistant design criteria. To support such assessments, earthquake catalogs typically include essential parameters such as epicenter location, focal depth, and magnitude[4–6]. Although numerical simulation, historical surveys, 1 g and hypergravity physics, and advanced machine learning methods can be employed to evaluate the geotechnical properties and the seismic disaster risk of relevant facilities, understanding the spatial and temporal characteristics of seismicity is particularly vital for delineating seismic zones, forecasting future earthquake trends, and informing targeted mitigation effort[7–12]. Despite variations in catalog completeness and magnitude scales, documenting both historically destructive earthquakes ($M \geq 4.7$) and modern regional earthquakes in Shandong (spanning 1484–2023 within 34.7°-38.5°N, 115.0°-119.5°E) provides a more robust perspective on the region's long-term seismic behavior.

In addition to seismic catalogs, detailed investigations of tectonic structures-including major faults, neotectonic activity, and earthquake focal mechanism solutions-are critical for characterizing the seismogenic environment[13]. Herein, we refer to these data collectively as "seismotectonic data", encompassing mapped faults, structural lineaments, and relevant focal mechanisms that together form the seismic structural framework of

[1]Ji'nan Communications Development & Investment Co., Ltd., Jinan 250101, China. [2]Department of Geotechnical Engineering, Tongji University, Shanghai 200092, China. [3]Department of Civil and Environmental Engineering, National University of Singapore, Singapore 117576, Singapore. ✉email: 2111373@tongji.edu.cn; xf.ma@tongji.edu.cn

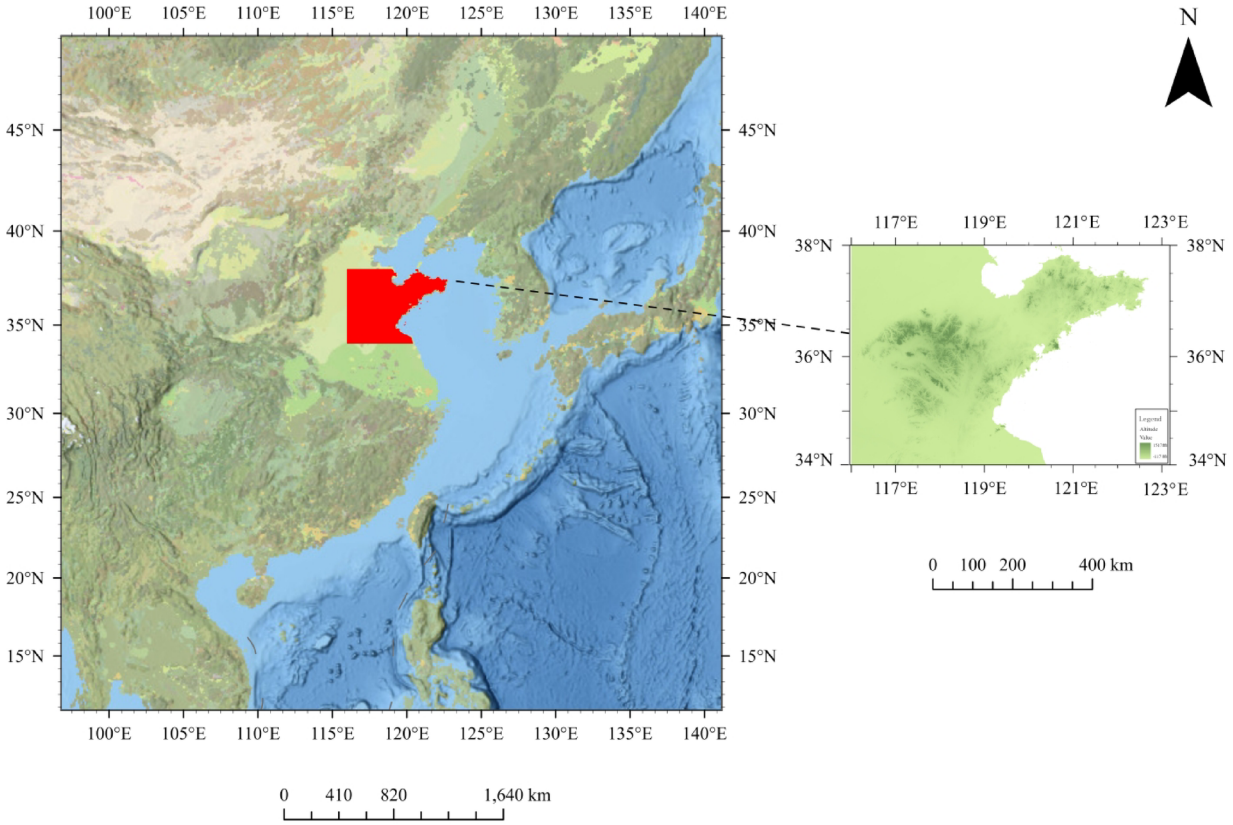

Fig. 1. Map of Shandong Region, between 116° to 123° east longitude and 34° to 38° north latitude. The red area represents the study area of this research – Shandong Region. Produced by GISPro (version 3.3.2; https://pro.arcgis.com).

Shandong. This framework reveals the geological setting and stress regimes that facilitate the occurrence of strong earthquakes, offering foundational insights for identifying likely epicentral zones and refining regional seismic hazard assessments.

This study aims to (1) compile and integrate comprehensive seismic and structural datasets for Shandong Province, (2) characterize the spatial and temporal patterns of earthquakes, and (3) investigate the tectonic features that underlie regional seismic activity. By synthesizing historical and modern earthquake catalogs with detailed fault and focal mechanism information, we provide a basis for improved earthquake source modeling and hazard assessment. Ultimately, these findings will aid in developing more precise seismic safety provisions and earthquake-resistant design standards to safeguard lives, property, and infrastructure against future earthquake disasters in Shandong.

Methods and technical validation

In this study, a comprehensive collection and review of seismic data were undertaken to establish a scientifically robust seismic catalog for the region. The methodology adhered to two key principles. Firstly, for destructive earthquakes that have been investigated and reviewed, the seismic parameters derived from these studies were directly incorporated. Secondly, the process included a critical evaluation of the reliability and completeness of multiple versions of catalog data, particularly for disputed earthquake records, to determine the most accurate and comprehensive entries for inclusion. Primary sources of seismic data utilized in this compilation included Seismic Damage Prevention Department of China Earthquake Administration, China Earthquake Administration Analysis and Forecast Network, and the official seismic catalogs issued by China Earthquake Network[13–16].

For seismic events with a magnitude equal to or greater than 4.7 ($M \geq 4.7$), those with available instrumental data are assigned magnitudes based on instrumental measurements. In cases where instrumental records are unavailable, earthquake magnitudes are estimated by analyzing historical accounts of epicentral intensity. These intensity values are then converted to approximate magnitudes through established empirical relationships between magnitude and epicentral intensity. Contemporary minor seismic events are typically characterized using M_L. The conversion equations utilized are sourced from "Earthquake Work Manual"[17].

$$M_s = 1.13M_L - 1.08 \quad (1)$$

The conversion equation was developed through a statistical analysis of Xingtai earthquake data by Guo et al. (1971). It is specifically designed for North China region and other areas where the epicentral distance Δ is less than or equal to 1000 km (Seismic Damage Prevention Department of National Earthquake Administration, 1990). In the process of creating the fifth series of seismic zoning maps, the correlation between M_s and M_L was re-examined using a substantial volume of modern earthquake data. By analyzing 6577 earthquakes that occurred between 1990 and 2007, with both M_s and M_L data available and focal depths below 70 km, the following M_s-M_L relationship was established as follows:

$$M_s = 0.932M_L - 0.295 \tag{2}$$

As shown in Fig. 2, the regression line of Eq. (1) exhibits a significant bias towards the dataset, whereas Eq. (2) aligns with the line M_s=M_L, with minor deviations observed at the extremes. Given the dispersion of data points and the significant uncertainty in the fitting relationship, it is generally accepted that Eq. (2) is fundamentally in agreement with M_s=M_L relationship. Because the M_L is saturated at approximately 6.5-7.0, in the statistical examination of seismic activity parameters, the modern M_L < 6.5 will be directly utilized as M without conversion to M_s. In determining the epicenter location, preference will be given to macroseismic epicenters for earthquakes with both instrumental and macroseismic epicenters. The analysis of the spatiotemporal characteristics of seismic activity will involve earthquake data with $M \geq 2.0$ since 1970. The seismic conditions pertaining to regional seismotectonics will be elucidated through an examination of medium earthquake occurrences in the region and its adjacent areas.

The region primarily encompasses North China Plain Seismic Statistical Area and Tancheng-Lujiang Seismic Statistical Area. A seismic statistical area refers to specific regions designated for conducting seismic statistical analyses. These areas are delineated based on geological structures and seismic activity characteristics to facilitate more accurate data collection and analysis. Based on earthquake records from these seismic statistical areas and research conducted by Huang et al.[57–59], historical records of destructive earthquakes have been largely comprehensive since 1484, with the exception of maritime areas. The northeastern section of the region includes Yellow Sea area, where a more in-depth analysis of seismic data completeness reveals relatively robust earthquake records. The earliest recorded destructive earthquake occurred in Laizhou Bay, Shandong in 1346, registering M = 5.0 and documented in five locations, including Yidu (Qingzhou), Changle, Shouguang, Weifang, and Jimo. In 1517, an M = 5.5 earthquake struck Yexian, located west of Laizhou Bay, Shandong, and was reported in ten locations, including Yidu, Jinan, and Yexian. The 1548 Bohai earthquake, measuring M = 7.0, was felt from Beijing in the west to Seoul on Korean Peninsula in the east, with over twenty counties documenting the event. Post-1500, earthquake records M > 5.0 in North Yellow Sea area are considered essentially complete, indicating that records of earthquakes M > 5.0 have been comprehensive since 1500.

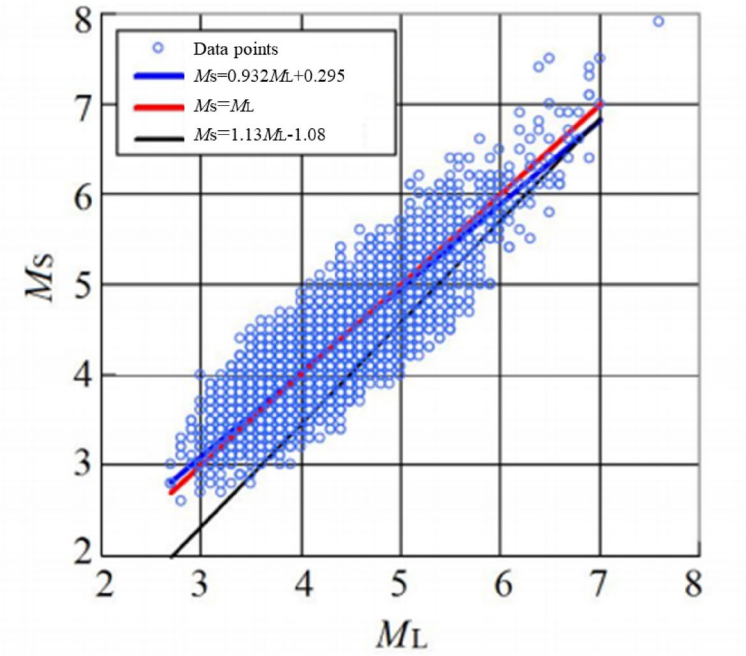

Fig. 2. The relationship of M_s-M_L. The blue circles represent data points, the blue line represents the conversion equation based on modern data, the red line represents the M_s = M_L conversion equation, and the black line represents the conversion equation developed for North China based on Xingtai earthquake data. The pattern does not align with the North China relationship, and the M_s =M_L equation is generally accepted as consistent with the derived relationship.

Most of the contemporary earthquake data from 1912 to the present have been collected through the use of seismic instrumentation. The first seismic observatory in Shandong, Tai'an Benchmark Seismological Station, was established in 1967. According to "Shandong Province Earthquake Catalog", between 1967 and 1980, 26 seismic stations were set up in Shandong, creating an initial regional seismic network with monitoring capabilities. Subsequently, starting from 1981, the layout and instrumentation of Shandong seismic network were improved. This involved the reconfiguration and addition of six seismic stations and Jiaxiang wireless transmission sub-network. These enhancements significantly improved earthquake monitoring in Shandong's inland areas, particularly in the southern region. With the exception of northern Shandong and parts of Jiaodong Peninsula, the earthquake monitoring capability in Shandong's inland areas is effective for $M \geq 2.0$, with southern Shandong capable of monitoring earthquakes down to $M \geq 1.7$. Post-1991, in response to the seismic activity characteristics in Shandong and adjacent regions and the evolving seismic conditions, Shandong seismic network was further expanded and optimized, increasing the number of stations to 32. Notably, with the development of digital observation technology, 19 digital observation stations were established by 2000, leading to the formation of Shandong Provincial Digital Seismic Network. This development significantly improved earthquake monitoring capabilities and positioning accuracy in Shandong's inland and nearshore areas.

Over the course of several decades of development and construction, the seismic monitoring capacity in various regions of Shandong has made significant advancements. In the western region and Yellow Sea area, the monitoring capability now enables the detection of earthquakes with $M \geq 1.7$. Similarly, the central and eastern regions have achieved a monitoring capability of $M \geq 1.4$. Specific areas such as Jiaodong Peninsula (e.g., Laizhou, Laiyang, Haiyang, and Rushan) and parts of Western Shandong (e.g., Jinan and Tai'an) have reached a monitoring capability of $M \geq 0.8$[18]. Henan, the seismic monitoring capability was $M \geq 2.5$ from 1970 to 1979 due to a limited number of stations. This capability improved to $M \geq 2.3$ from 1980 to 2001 during a period of relatively stable analog observation. However, from 2002 to 2007, the discontinuation of several analog observation stations resulted in significant gaps in earthquake records, with monitoring capability approximately $M \geq 2.6$. Subsequently, from 2008 to November 2020, the seismic monitoring capability increased to $M \geq 1.5$ following the completion of the seismic network's digital upgrade and the deployment of new stations, thereby enhancing monitoring capabilities significantly[19]. The Hebei digital seismic network, post "Eleventh Five-Year Plan" project transformation, has achieved earthquake monitoring of $M \geq 1.5$ across most of the province[20]. However, there remains insufficient station density in Hebei's border areas, affecting monitoring capabilities. According to Mou et al. (2016)[42], the entire Hebei region is capable of monitoring earthquakes with $M \geq 2.5$.

In summary, considering the seismic networks of both regional and neighboring countries, as well as provincial seismic networks, the earthquake monitoring capability in the region is generally effective for events $M > 2.0$, with certain areas even capable of detecting earthquakes as low as $M = 1.0$. Analysis of data from different time periods, dating back to 1970, suggests that there might have been instances where earthquakes $M \approx 2.0$ were missed during specific intervals. However, on the whole, the documentation of earthquakes $M \geq 2.0$ is considered to be comprehensive and dependable.

Regional seismic activity analysis

Seismic records indicate that the earliest earthquake in the region was $M = 7.0$ earthquake in Anqiu, Shandong, in 70 BC[21], with the largest being July 25, 1668, Tancheng, Shandong, earthquake $M = 8.5$ with an intensity of XII[21–24]. The most recent earthquake of $M \geq 4.7$ was a $M = 5.5$ earthquake in Dezhou Plain, Shandong, on August 6, 2023. Table D-1 in the supplementary database compiles the catalog of regional destructive earthquakes (70 BC-December 2023, $M \geq 4.7$), and Table 1 presents the statistics of earthquake magnitudes for regional destructive earthquakes. To ensure the quality of seismic data compilation, we employed stringent numerical screening and verification standards, conducting a comprehensive evaluation of factors such as magnitude, depth, moment tensor solutions, station coverage, and observational geometry. This approach enhances the reliability and completeness of the database. Any events that do not meet the minimum acceptable thresholds or exhibit significant conflicts in data consistency are excluded.

In Table 1, spanning the period from 70 BC to December 2023, there were a total of 115 documented earthquakes with $M \geq 4.7$ within the specified region. These earthquakes were further categorized as follows: 37 events with $4.9 \geq M \geq 4.7$, 55 events with $5.9 \geq M \geq 5.0$, 17 events with $6.9 \geq M \geq 6.0$, 5 events with $7.9 \geq M \geq 7.0$, and 1 earthquake with $M \geq 8.0$.

The earliest recorded modern earthquake in the region with $4.6 \geq M \geq 4.0$ was $M = 4.6$ earthquake in Bohai Sea on May 16, 1970[25,26]. The most recent earthquake $M > 4.0$ was $M = 4.3$ earthquake in Zibo, Shandong, on May 2, 2022. Table D-2 in the supplementary database summarizes the catalog of modern regional earthquakes (1970-December 2023, $4.6 \geq M \geq 4.0$), and Table 2 provides statistics for modern regional earthquakes (1970-December 2023, $M \geq 2.0$).

Magnitude categories (M)	Number of earthquakes
4.7–4.9	37
5.0-5.9	55
6.0-6.9	17
7.0-7.9	5
8.0-8.9	1

Table 1. Frequency distribution of regional destructive earthquake magnitudes (70 BC-December 2023, ≥ 4.7).

Magnitude categories	Number of earthquakes
2.0-2.9	3943
3.0-3.9	592
4.0-4.6	39

Table 2. Statistical distribution of modern regional earthquake magnitudes (1970-September 2023, $4.6 \geq M \geq 2.0$).

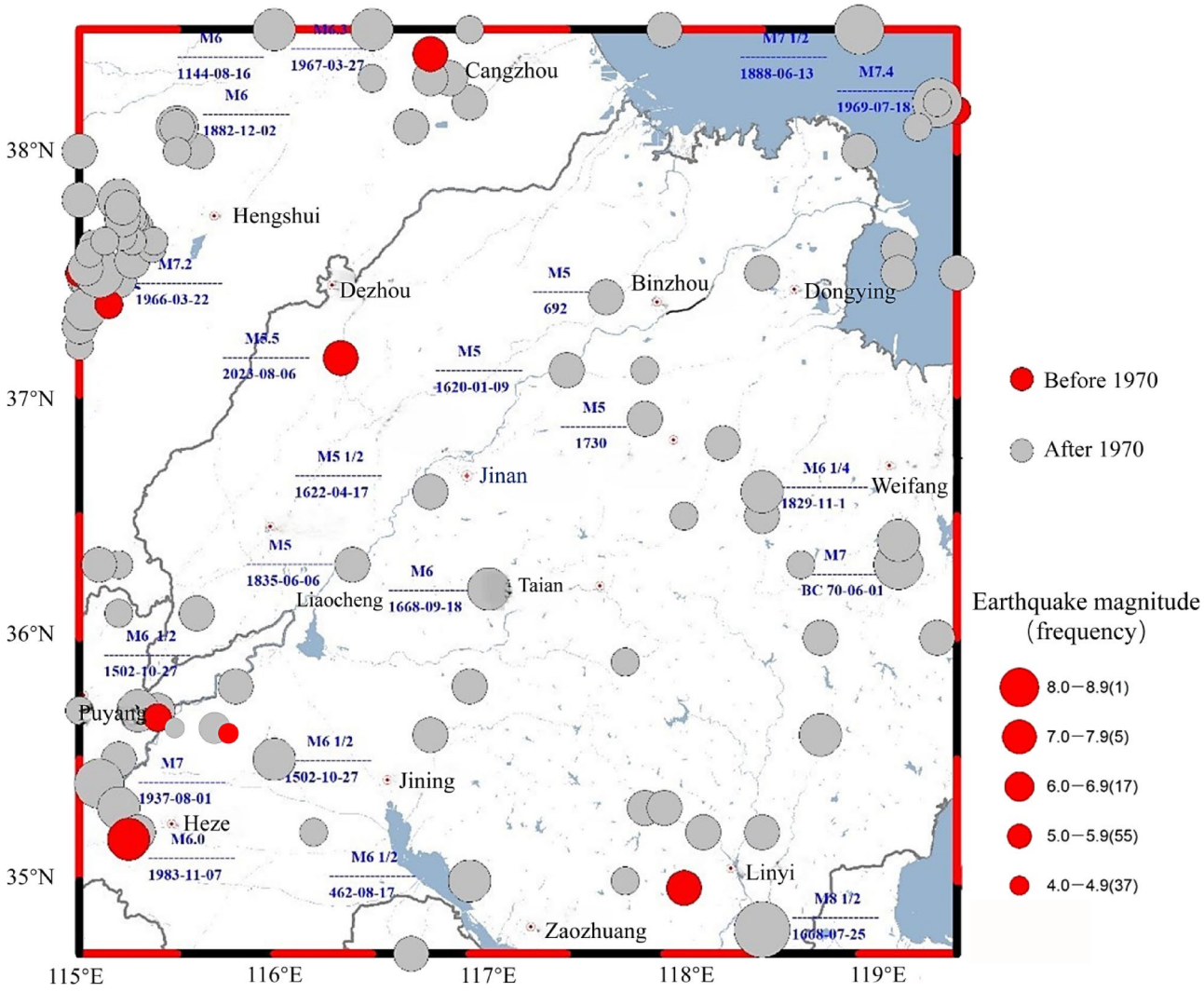

Fig. 3. Epicenter distribution of regional destructive earthquakes (70 BC to December 2023, $M \geq 4.7$). Red circles represent earthquakes that occurred before 1970, while gray circles denote those occurring after 1970. The size of red circles corresponds to the magnitude of the earthquakes. The maps were generated using maPInfo software (version 16; http://www.precisely.com) and modified using Power Point (version 2019; https://www.microsoft.com).

Based on the catalogs of regional destructive earthquakes ($M \geq 4.7$) and modern regional earthquakes ($M \geq 2.0$), Epicenter Distribution Maps for Regional Destructive Earthquakes (Fig. 3) and Epicenter Distribution Maps for Modern Regional Earthquakes (Fig. 4) were prepared to illustrate the spatial distribution characteristics of regional seismic activity. In the process of data compilation and selection, we primarily relied on seismic information recorded by monitoring stations. The catalog of regional destructive earthquakes ($M \geq 4.7$) from 70 BC to December 2023 has been compiled in Table D-1, while the catalog of modern regional earthquakes ($4.6 \geq M \geq 4.0$) from 1970 to December 2023 is summarized in Table D-2. The data were sourced from rigorously validated and certified seismic networks, utilizing high-quality observational data to ensure accuracy and reproducibility. This study focuses on the specific geographical region defined between 34.7° and 38.5° North

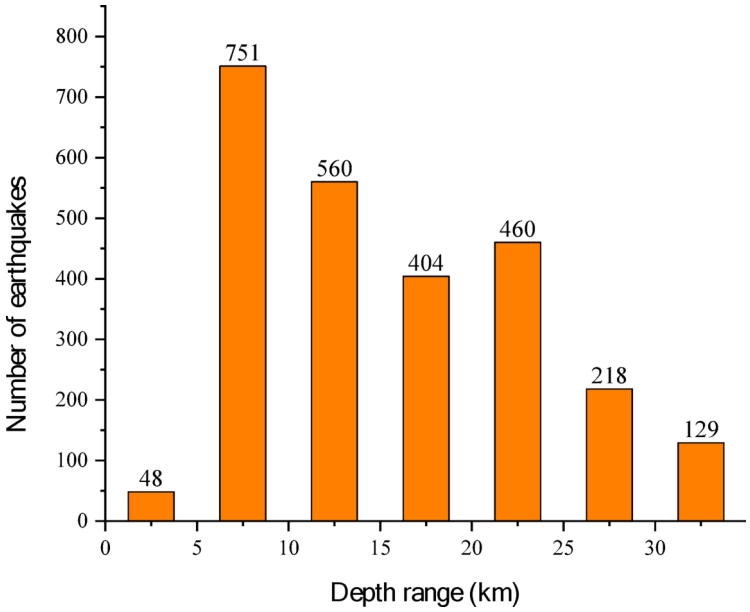

Fig. 4. Histogram of focal depths for modern regional earthquakes (January 1970 to December 2023, 2.0 ≤*M*≤ 4.6). The numbers on the histogram represent the number of earthquakes that occurred.

latitude and 115.0° to 119.5° East longitude. Additionally, longitude and latitude labels have been included in the figures to facilitate precise localization within this area.

We have systematically integrated seismic records from historical documents and archaeological findings, including ancient texts describing past earthquakes and evidence of seismic damage unearthed at archaeological sites. However, over an approximate period of 2000 years, only 55 earthquake events fell within the *M* 5.0–5.9 range, largely due to historical variations in seismological station density and the overall development of the regional monitoring network. In earlier centuries, particularly before modern instrumentation, earthquake detection relied on a limited and geographically dispersed network of observers. By contrast, the establishment and expansion of modern seismological networks in the latter half of the 20th century have significantly enhanced the recording of smaller-magnitude earthquakes-evidenced by Table 2, which shows a considerable rise in recorded events within the*M* 4.0–4.6 range from 1970 to December 2023, including 3943 *M* 2.0–2.9 events. This surge reflects improved observational capabilities and denser station coverage, indicating that the low count of moderate earthquakes in historical catalogs stems primarily from observational constraints rather than a genuine scarcity of seismic activity. Furthermore, early records were incomplete due to a lack of systematic documentation in ancient societies, limited or inaccessible areas left unrecorded, and inconsistencies across different sources. Socioeconomic factors also played a role: during periods of lower societal and technological development, earthquake documentation was scarce, whereas modern advancements in monitoring networks and reporting practices have led to broader and more accurate record-keeping. Consequently, smaller and moderate earthquakes may be underrepresented, potentially underestimating overall seismic activity and affecting risk assessments. Thus, the incompleteness of early seismic catalogs should be interpreted with caution, acknowledging the impact of temporal changes in network density. Future seismic hazard evaluations should account for these observational biases to achieve a more accurate understanding of the region's long-term seismicity. We will continue supplementing our database with new historical and archaeological discoveries to minimize these data gaps.

Figure 3 depicts the distribution of epicenters for regional destructive earthquakes. The spatial pattern of these earthquakes demonstrates significant heterogeneity. Specifically, areas with higher frequency of destructive earthquakes are observed along the southern segments of Xinhe and Liaocheng-Lankao fault zones, which have experienced multiple regional earthquakes $M > 6.0$. The seismic activity in the northwestern faults of Yihe River-Shuhe River fault zone and West Shandong block impacts the region, especially at the intersections of active faults, making these areas particularly susceptible to earthquakes. Additionally, intense earthquakes were recorded within Bohai Basin. The faults mentioned in the text can be found in Fig. 8.

A total of 115 destructive earthquakes were documented in the region, with focal depth information accessible for 40 of these events, averaging a focal depth of 19.0 km. To conduct a more detailed analysis of the earthquake focal depths in the region, 2570 earthquakes with depth data and $M \geq 2.0$ were chosen. The analysis of earthquake focal depths (Figs. 4 and 5) indicates an average focal depth of 14.9 km for the 2,570 recorded earthquakes, which is slightly shallower than the average depth of destructive earthquakes. The majority of these events occur at depths less than 30 km, accounting for approximately 95% of the total seismic activity. Specifically, earthquakes occurring at depths within 15 km comprise 51.9% of the total, while those between 15 km and 20 km represent 26.4%. These results demonstrate that seismic events in the region predominantly originate in the upper to middle crust, classifying them as shallow-focus earthquakes.

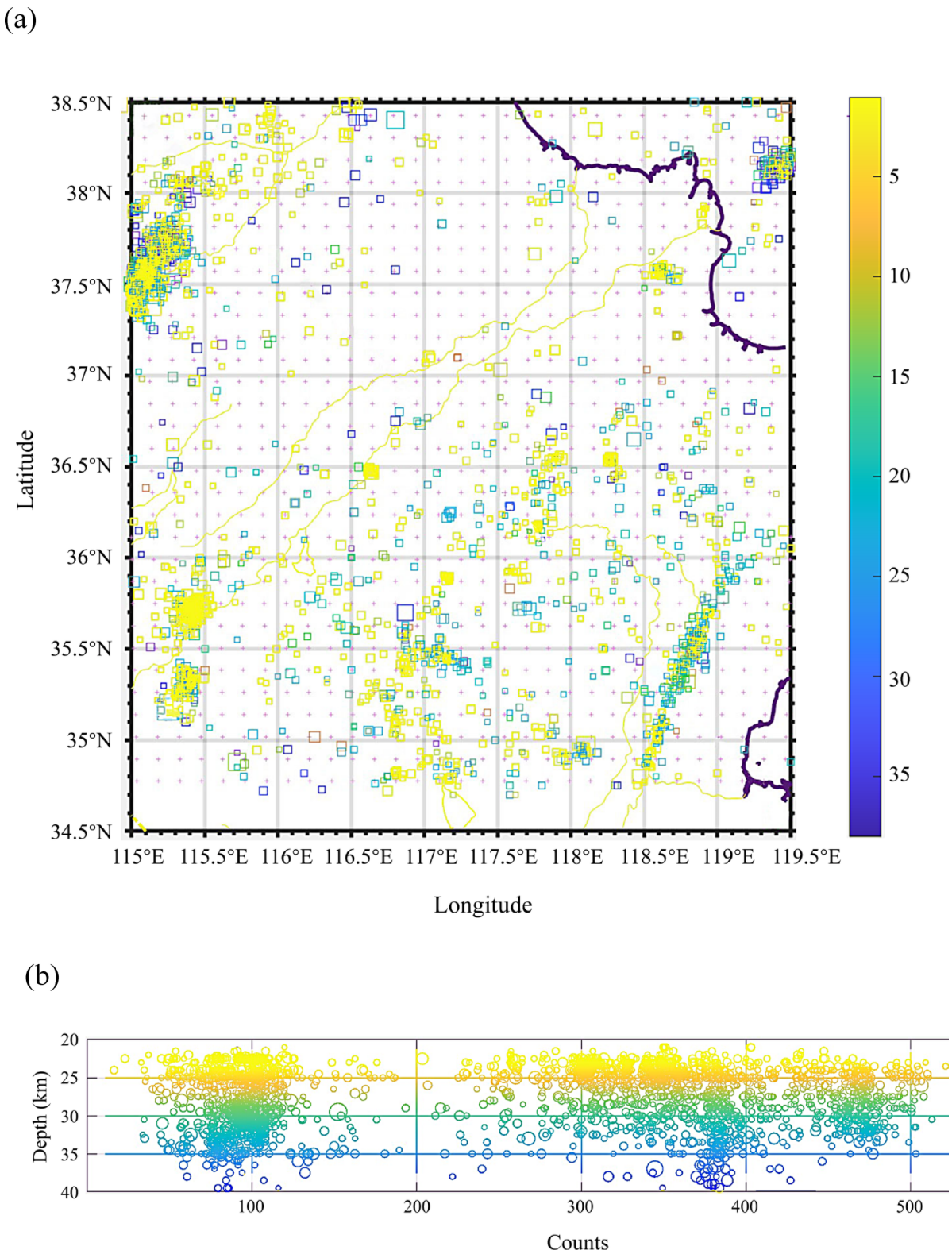

Fig. 5. Focal Depth Profile of Modern Regional Earthquakes (January 1970 to September 2023, 2.0 ≤*M*≤ 4.6). (**a**) Hypocentral Depth-Azimuth Map. (**b**) Hypocentral Depth-Quantity Chart. Each square in the figure (a) represents an earthquake, with the color indicating the depth, transitioning from blue to yellow as the seismic source depth gradually increases. The figure (b) records the number of earthquakes at different depths, with the color change reflecting the increasing depth of the seismic source. The maps were generated using maPInfo software (version 16; http://www.precisely.com) and modified using Power Point (version 2019; https://www.microsoft.com).

Figure 6 presents an Magnitude-Time (M-T) diagram illustrating regional destructive earthquakes. Before 1485, there were limited records of destructive earthquakes, resulting in significant data gaps. After 1485, regional earthquakes exhibit evident periodicity, aligning with statistical data from North China Plain seismic area. The region experienced periods of heightened seismic activity between 1485 and 1675 and 1791–1983, characterized by a higher frequency of recorded destructive earthquakes. These intervals suggest alternating phases of intensified and subdued seismic activity. Following 1983, the region entered a relatively quiescent phase, with the most significant recent event being M= 5.5 event in Shandong Plain (2023).

.

Seismic activity exhibits spatial heterogeneity, with medium and strong earthquakes, particularly those with M = 6.0 and higher, being affected by active fault zones and distributed in zones along these faults. Statistical results indicate that the average focal depth of regional destructive earthquakes is 19 km, while the average focal depth for recent minor earthquakes is 14.9 km. Regional earthquakes are predominantly located in the middle to upper crust and are categorized as shallow-source earthquakes. The area mainly encompasses North China Plain Seismic Statistical Area and Tancheng-Lujiang Seismic Statistical Area[27,28]. Over the next century, the seismic activity in North China Plain Seismic Statistical Area is projected to persist at or above the long-term average level. In contrast, Tancheng-Lujiang Seismic Statistical Area should account for seismic activity reflective of its average levels during historically active phases. The region is currently in the fourth active phase of North China seismic cycle, with a conservative estimate suggesting the potential occurrence of earthquakes with magnitudes approaching $M \approx 7.0$ occurring in the next 100 years.

After systematically reviewing the spatiotemporal distribution characteristics and activity levels of earthquakes in this region, it becomes evident that moderate to strong earthquakes are frequently associated with major fault zones or block boundaries, particularly at the intersections of multiple faults or the termini of active fault segments, where high-magnitude events are more likely to occur. This uneven spatial distribution and the periodicity observed in the temporal sequence are intrinsically linked to the regional geological structures and neotectonic movements. On one hand, differential movements along significant deep-seated faults and block boundaries provide essential mechanical environments for the accumulation and release of crustal stress. On the other hand, the juxtaposition and displacement between faults of varying orientations can influence earthquake source processes and rupture patterns to some extent.

Therefore, following the assessment of seismic activity, it is crucial to further analyze the geological structural background, characteristics of neotectonic movements, and the distribution of the modern stress field in this region to understand the conditions and mechanisms underlying earthquakes of various magnitudes. By integrating structural factors such as the orientations of major faults and fault activity attributes with seismic activity data, the controlling effects of geological structures on earthquake occurrence can be more clearly elucidated.

Regional seismic structural characteristics

The occurrence of earthquakes is closely linked to specific geological backgrounds, particularly the association between earthquakes of M = 6.0 and higher with significant fault activity and deep structural variations. Therefore,

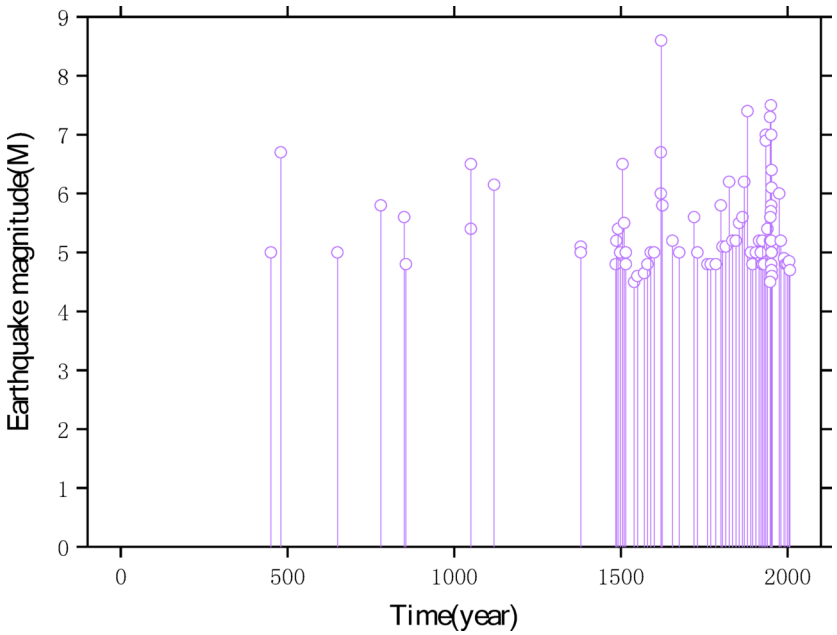

Fig. 6. M-T diagram for regional destructive earthquakes. The picture intuitively reflects the variation of earthquake activity over time. The denser the purple line, the higher the frequency of seismic activity during that period.

the analysis of regional geotectonic backgrounds and seismic geological features, along with the identification of structural indicators for powerful earthquakes, not only serves as a foundation for defining seismic zones, belts, and potential epicentral areas but also holds significant importance for the comprehensive evaluation of seismic risk at various sites. The development of a comprehensive regional seismotectonic database relied on existing datasets[29–32], supplemented by extensive field geological surveys. This effort emphasized the examination of regional geotectonics, neotectonic activities, major fault characteristics, and fault activity. Additionally, the process involved creating detailed regional seismic structural maps. These analyses illuminate the seismic structural framework and tectonic conditions that favor the occurrence of strong earthquakes, providing a foundational basis for identifying potential epicentral zones and refining seismic hazard assessments.

In Table 3; Fig. 7, the regional analysis primarily encompasses West Shandong Block, Eastern Hebei-Bohai Block, Zuzhou-North Huaihe River Block, Jiaodong Peninsular-Liaodong Peninsula Block, and Northern Jiangsu-Jiaonan Block within Yangtze Block area[33–36]. The majority of these regions fall within North China Block and Yangtze Block areas.

North China Block Region is characterized as one of the oldest stable areas in China, exhibiting a distinctive double-layer structure. The basement comprises Archean and Lower Proterozoic medium to deep metamorphic rock systems, which were consolidated by Lvliang Movement[37,38]. Middle and Upper Proterozoic periods are associated with Yanshan-Taihang Mountains ancient rift valley sedimentary system. Throughout Paleozoic to Triassic periods, the region experienced relatively stable platform cover layer sedimentation. Yanshan Movement, marked by intense activity, led to the formation of primarily northeast-oriented folds, thrust faults, and magmatic belts. Subsequently, during Cenozoic era, the platform underwent further disintegration, resulting in the formation of fault depressions and uplifts in North China Plain and Bohai Sea area, controlled by north-northeast-oriented and northwest-west-oriented faults. The boundaries of North China Block Region are delineated by significant deep faults. Internally, North China Block exhibits a structural and geomorphic pattern characterized by alternating northeast-oriented uplifts and subsidence areas. This alternating pattern of uplifts and subsidence has persisted since the neotectonic period, affecting the distribution of earthquakes within North China Block[39,40].

Yangtze Block Region is predominantly situated on both sides of Yangtze River Basin, stretching eastward from the coastal areas of Jiangsu across Southern Yellow Sea into Southern Korea. Its boundaries are delineated by deep lithospheric fault zones, which separate it from neighboring geotectonic regions. The formation and evolution of Yangtze Block Region have unfolded over an extensive geological timeline, encompassing the development phase of Pre-Sinian Jinning trough and the platform evolution from Sinian to Quaternary period[41–43]. The former phase laid the groundwork for the block's basement, while the latter phase contributed to the formation of the block's cover layer, separated from the basement by a regional unconformity. The pre-Sinian basement of Yangtze Block Region comprises a series of sedimentary-metamorphic rocks exhibiting diverse structural lithofacies characteristics, predominantly located at significant depths below the surface, with certain exposures present along the current peripheral uplift zones and specific uplift areas within the block[44].

The regional neotectonic movement in the area is marked by intense activity, with differential movements of blocks and fault actions showing dextral oblique-slip along north-northeast-oriented faults and sinistral oblique-slip along northwest-oriented faults[45]. The neotectonic zoning and features mentioned above suggest that the movements in this region are a combination of inherited and newly developed processes, displaying periodicity over time and variations in spatial tilting. Three fundamental characteristics can be summarized as follows:

Intermittent and general uplift and subsidence

Since Neogene period, the central and eastern Shandong mountains have experienced extensive, intermittent uplift, resulting in the formation of complex geomorphological features, including four levels of planation surfaces. Within these mountainous regions, three levels of river terraces have developed, while the coastal zones exhibit five levels of marine erosion terraces. Concurrently, the eastern basins of North China region have undergone significant subsidence, leading to prominent sedimentary discontinuities between Oligocene and Miocene epochs, as well as between Pliocene and Quaternary periods. Neogene and Quaternary strata within these basins exhibit thicknesses ranging from several hundred meters to over one thousand meters and are characterized by numerous sedimentary cycles and multi-phase accumulations. These results underscore the region's dynamic history of episodic uplift and subsidence.

Differential and tilting activities of fault blocks

The data on mountain altitudes, planation surface elevations, and basin sediment thicknesses highlight substantial variations in the magnitudes of uplift and subsidence across different geological blocks, accompanied by different tilting characteristics. For instance, uplifted regions within Neogene uplift framework, such as the

First-level unit	Second-level unit
North China Block Region (I)	West Shandong Block (I_1)
	Eastern Hebei-Bohai Block (I_2)
	Zuzhou-North Huaihe River Block (I_3)
	Jiaodong Peninsular-Liaodong Peninsula Block (I_4)
Yangtze Block Region (II)	Northern Jiangsu-Jiaonan Block (II_1)

Table 3. Summary of regional geotectonic zoning.

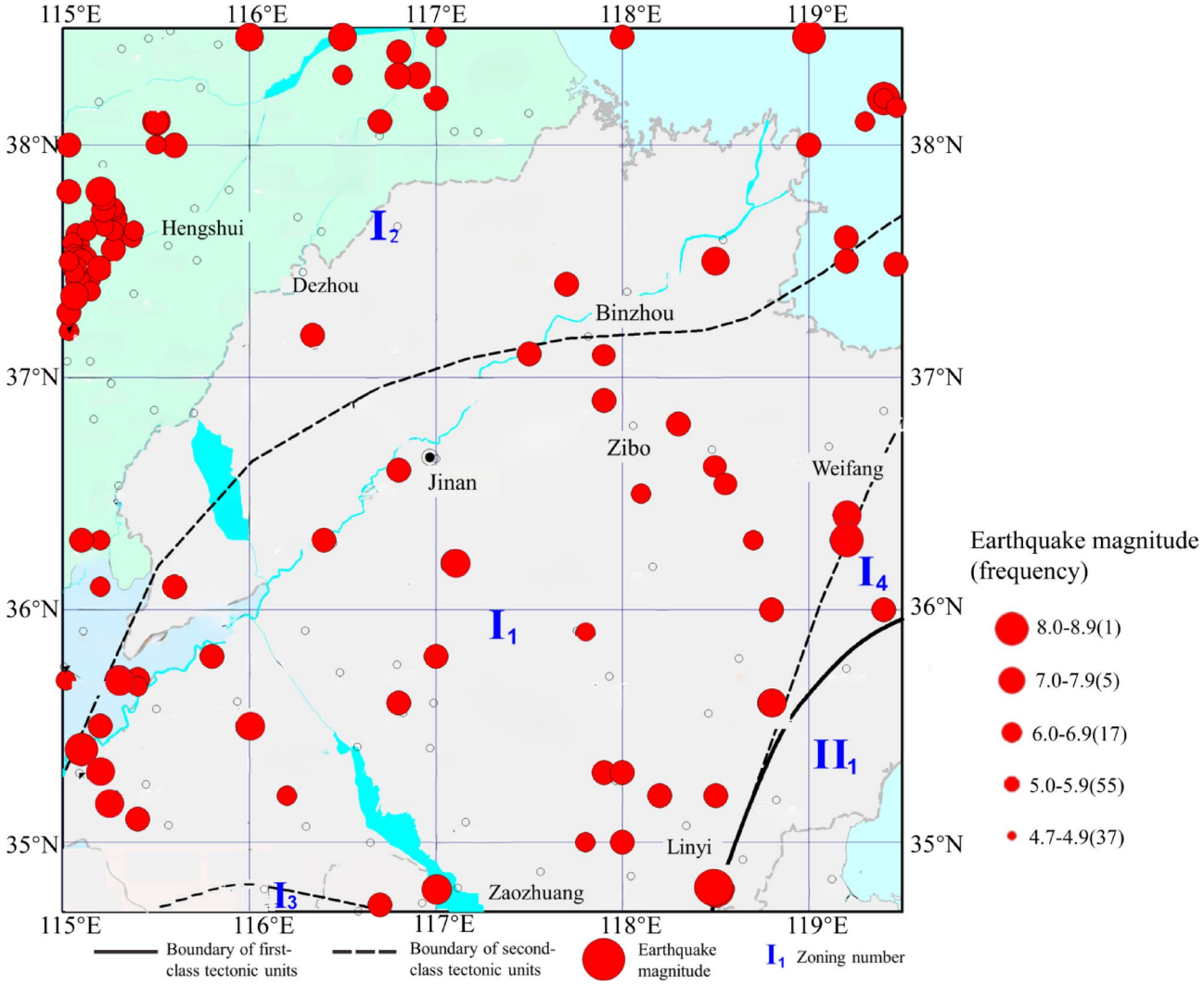

Fig. 7. Regional geotectonic zoning. The Roman numerals in the figure represent different blocks. I. North China Block Region; I_1. West Shandong Block; I_2. Eastern Hebei-Bohai Block; I_3. Zuzhou-North Huaihe River Block; I_4. Jiaodong Peninsular-Liaodong Peninsula Block; II. Yangtze Block Region; II_1. Northern Jiangsu-Jiaonan Block. The maps were generated using maPInfo software (version 16; http://www.precisely.com) and modified using Power Point (version 2019; https://www.microsoft.com).

southern central and eastern Shandong uplift, display a pronounced southward tilt. These tilting movements are primarily driven by the normal slip of faults within the basins, resulting in the formation of tilted fault depressions on the downthrown sides and uplifted fault blocks on the upthrown sides.

Inheritance and neoteny of fault and block activities

Fault and block movements in the region have largely inherited pre-existing structural patterns and modes of activity, with differentiation during Xishan Movement playing a pivotal role in shaping these configurations. This influence is particularly pronounced in the neotectonic period, beginning in the Quaternary. During this time, uplifted areas have continued to experience elevation, while subsided regions have undergone further depression. Additionally, fault and block activities exhibit characteristics of neoteny, as evidenced by intervals within the neotectonic period where faults and blocks display reverse movements or new structural blocks emerge along pre-existing fault lines and boundaries.

In Table 4, the region can be subdivided into 4 secondary zones and 13 tertiary zones based on factors such as developmental history, types, magnitudes, geomorphic features, main controlling faults' orientations and activities, and seismic activity.

Regional neotectonic movements are predominantly defined by the differential uplift and subsidence of fault blocks, driven by fault activity. Destructive earthquakes often originate in structural settings where these differential movements are particularly pronounced, commonly leading to the formation of fault depression basins. Strong earthquakes are frequently concentrated in specific structural features within these basins, such as the steeply dipping flanks of tilted fault basins, zones with significant fault displacement, transverse uplifts within

Primary neotectonic zone		Secondary neotectonic zone		Tertiary neotectonic zone	
Number	Name	Number	Name	Number	Zone name
I	North China Neotectonic Zone	I-1	Eastern North China Basin Fault Depression Zone	I-1-1	Central Hebei fault depression
				I-1-2	Cang County fault uplift
				I-1-3	Huanghua fault depression
				I-1-4	Chengning fault uplift
				I-1-5	Jiyang depression
				I-1-6	Xingtai-Hengshui fault uplift
				I-1-7	Linqing fault depression
				I-1-8	Neihuang fault uplift
				I-1-9	Dongpu depression
		I-2	West Shandong Block Uplift Zone	I-2-1	West Shandong Northern Subsidence slope belt
				I-2-2	Southern Central Shandong strong fault uplift
				I-2-3	West Shandong Southern fault depression
		I-3	Eastern Shandong Block Uplift Zone	I-3-1	Jiaonan Weak fault uplift
		I-4	Tancheng-Lujiang Fault Zone Active Area		

Table 4. Regional neotectonic zoning.

basins, apex areas of triangular fault basins, secondary grabens within composite fault systems, and intersections of multiple active fault lines. This pattern is evident in historical events such as the 1937 Heze M= 7.0 earthquake, the 1966 Ningjin M = 7.2 earthquake, and the 1622 Yuncheng M = 6.0 earthquake[46–48]. Strong earthquakes are commonly observed at the terminations of active faults or at intersections of two or more active structural belts, as exemplified by the 1668 Tancheng M = 8.5 earthquake and the 70 BC Anqiu M = 7.0 earthquake in Shandong.

The region features a network of prominent large-scale faults, predominantly oriented in a northeast-north-northeast direction, followed by northwest-northwest-west orientations, with a smaller subset trending nearly east-west. These fault systems include the southern section of Tangshan-Hejian-Cixian Fault Zone, faults within Eastern North China Basin fault depression zone, Tancheng-Lujiang Fault Zone, and faults located in West Shandong Block region, along with specific faults in Southern Yellow Sea. Figure 8 summarizes the primary fault structures within the region, while detailed attributes (e.g., fault length, strike, dip direction, dip angle, fault type, determination methods, latest periods of activity, and historical earthquake records) are provided in the supplementary database Table D-3.

The contemporary tectonic stress field is essential for investigating the circumstances leading to significant earthquakes, facilitating the examination of fault activity and types of slip[49]. The statistical properties of the primary stress axes orientations derived from focal mechanism solutions can depict the key aspects of the regional contemporary tectonic stress field. Therefore, the utilization of focal mechanism data enables a more in-depth analysis of the features of the regional contemporary tectonic stress field and the characteristics of the source faulting. Through the inversion of the modern tectonic stress field for mainland China, particularly in Eastern China and North China, based on focal mechanism solutions from a series of recent strong and moderate-to-minor earthquakes, numerous researchers in China have conducted studies. In Eastern China, especially for earthquakes with $M \geq 6.0$, the dip angles of the two nodal planes of the focal mechanisms typically range between 60° and 70°, with the principal compression stress axis predominantly oriented near-horizontal, mainly towards the northeast, north-northeast, or almost east-west directions, gradually shifting from north-northeast to nearly east-west and northwest-southeast directions towards the south, primarily north-northeast in North China above latitude 34°N. The principal tension stress axis transitions from north-northwest to near north-south to north-northeast as one moves southwards, predominantly exhibiting north-northwest to near north-south orientations in North China above latitude 34°N; the dip angles of both the principal compression and tension stress axes are generally below 20°, with the force acting horizontally or nearly horizontally. This suggests that the current modern tectonic stress field in North China region is characterized by east-northeast to west-southwest compression and north-northwest to south-southeast extension. According to by Zhou et al.[50–52], the average orientation of the P axis in the comprehensive mechanism solution for Shandong is 76°, and the T axis is 345°; the average dip angles of P and T axes are both below 10°; the predominant orientations of P and T axes in individual earthquake focal mechanism solutions are approximately 80° and 340°, respectively; approximately 2/3 of P and T axes have dip angles within 30°; the principal compression stress axis direction in the modern tectonic stress field of Shandong is east-northeast, approximately 70° to 80°, and the principal tension stress axis orientation is north-northwest, approximately 340° to 350°. The force acts horizontally or nearly horizontally. The general characteristics of the stress field in Shandong are largely in line with the broader North China regional stress field.

Research has gathered and systematized focal mechanism solution data for moderate and minor earthquakes, as well as recent strong earthquakes in the region. This data serves as the foundational information for inferring and inverting the regional tectonic stress field. Details such as earthquake date, epicenter location, strike, dip direction, and dip angle of plane A, strike, dip direction, and dip angle of plane B, orientation and elevation angle of the P axis, and orientation and elevation angle of the T axis, are available in the supplementary database Table D-3 and Table D-4. As shown in Fig. 9, through statistical analysis of the regional data, a comprehensive

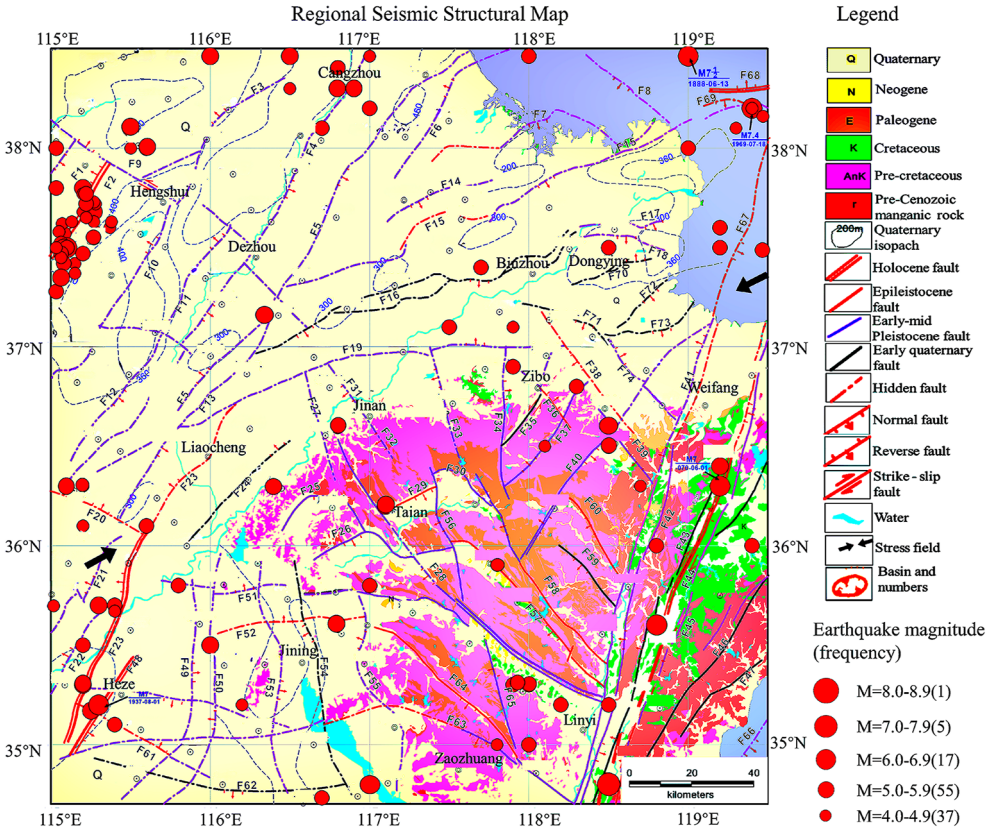

Fig. 8. Regional seismic structural map. This image summarizes the major fault structures in the region, with F1-F70 being the main faults in the region. The 'F' labels on the map represent different fault zones. Red circles represent earthquakes, and size of red circles corresponds to the magnitude of the earthquakes. Specific information can be found in the supplementary database Table D-3. The maps were generated using maPInfo software (version 16; http://www.precisely.com) and modified using Power Point (version 2019; https://www.microsoft.com).

mechanism solution was obtained, revealing an average P axis orientation of 76° and a T axis orientation of 345°. The average dip angles of the P and T axes are both below 10°, with the predominant orientations of the P and T axes in individual earthquake focal mechanism solutions being approximately 80° and 350°, respectively. In the region, the primary distribution orientation of the principal compression stress P axis is east-northeast, ranging between 60° and 90°, while the main orientation of the principal tension T axis is north-northwest, between 330° and 350°. However, the complex rose diagram suggests that local stress fields exhibit certain variance from the broader regional stress field. By integrating the analysis of the tectonic stress field in Shandong, the direction of the principal compression stress is identified to be between 60° and 90°, and the principal tension stress direction between 330° and 350°, aligning closely with the orientation of the larger North China regional tectonic stress field.

Based on the data presented above, the region is predominantly situated within a contemporary tectonic stress field characterized by a near east-northeast to west-southwest oriented near-horizontal principal compression stress and a near north-south oriented near-horizontal principal tension stress. In such a stress regime, there is a significant probability of strike-slip or a combination of strike-slip and dip-slip fault activities taking place. Examination of the two nodal planes and *P* and T axes from the focal mechanism solutions indicates that right-lateral strike-slip is probable on north-east oriented faults, whereas left-lateral strike-slip is anticipated on north-west oriented faults.

Based on the regional geological structure, neotectonic movement characteristics, modern crustal movement features (which refer to the patterns and rates of crustal movements recorded since 1970 through advanced seismic monitoring equipment and crustal deformation observation technologies), and their relationship with seismic activity, the seismic structural conditions for earthquakes of different magnitudes are summarized as follows: (1) For earthquakes $M \geq 8$, seismic structural indicators include earthquakes occurring along the boundaries of active geotectonic blocks, generally active deep major fault zones, such as the 1688 Tancheng-Lujiang fault zone Tancheng $M = 8.5$ earthquake. The causative fault shows clear Holocene activity signs, and the seismotectonic is often at the intersection of two groups of active structural belts. Numerous $M = 8$ earthquakes are related to areas with the largest vertical movements since Quaternary; (2) For earthquakes $7.9 \geq M \geq 7.0$, seismic structural indicators include areas with seismic structural indicators for $M \geq 8.0$ earthquakes, such as 70 BC Tancheng-Lujiang fault zone Anqiu $M = 7.0$ earthquake in Shandong. These earthquakes occur within large

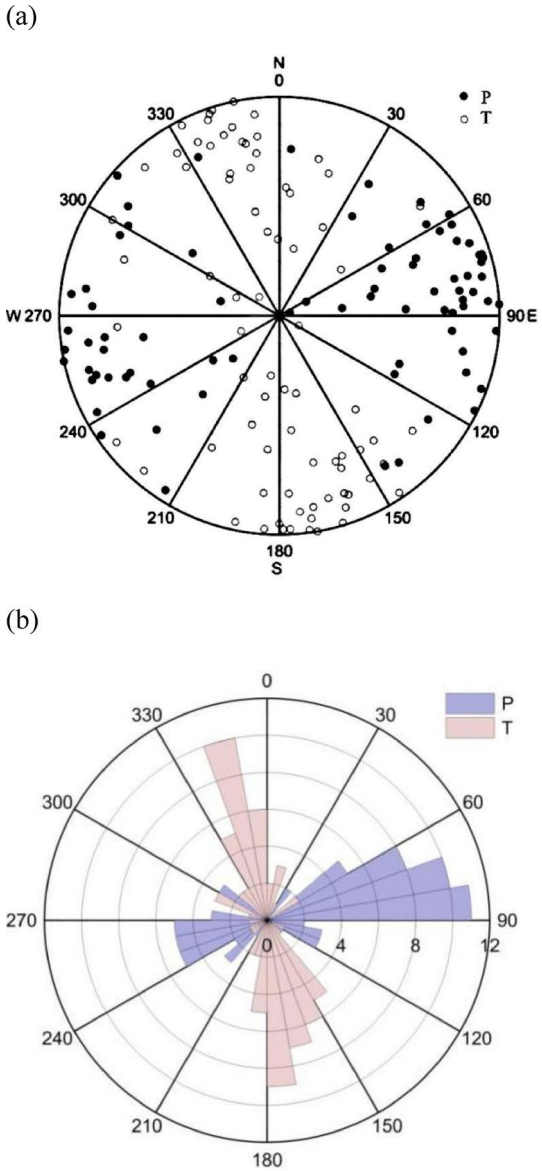

Fig. 9. Stereographic projections of *P* and *T* Axes for Regional Earthquakes ($M \geq 2.0$). (**a**) P and T Axes Stereographic Projection. (**b**) Orientation Stereographic Projection. The picture shows the azimuth and elevation information of the P-axis and T-axis, and this azimuth rose diagram reflects the geological characteristics of the area, indicating certain differences between the local stress field and the large-scale regional stress field.

depressions and uplift units controlled by major faults, such as 1888 Bohai Bay M = 7.5 earthquake and 1969 Bohai M = 7.4 earthquake. They also occur along major fault zones in North China Plain with clear Holocene activity, such as 1966 Hebei Xingtai M = 7.2 earthquake, and at the intersection of large active fault zones and active faults within West Shandong Block Basin, such as the 1937 Heze M = 7.0 earthquake. On 6th February 2023 (UTC), two consecutive and catastrophic earthquakes with moment magnitudes (*Mw*) 7.8 and 7.7 struck the Maras Triple Junction (MTJ) region. These events are likely associated with conventional fault activations, recurrence intervals, and seismic gaps[53]. The Lakes Van and Erçek regions suffered a NE-propagating sequence of blind thrust mainshock-aftershocks in the October 23, 2011 Van earthquake, *Mw* 7.1. This large blind thrust event ruptured the faults located within the accretionary prism, accumulated by the continent-continent collision between the Arabian and Anatolian plates[54]. (3) For earthquakes $6.9 \geq M \geq 6.0$, seismic structural indicators include not only being limited to Cenozoic active block boundary faults, boundary faults between uplifts and depressions, or Cenozoic intensely active basement faults. The causative fault is late Pleistocene and Holocene active faults, with diverse seismotectonic directions. These earthquakes commonly occur at junctions between secondary uplifts and depressions within structural blocks or at fault intersections, such as the 1829 Yidu M = 6.25 earthquake and the 2020, Elazig M = 6.8 earthquake[55]; (4) For earthquakes $5.9 \geq M \geq 5.0$, no different pattern in seismic structural conditions is observed. However, these events are linked to fault activity

and basin structural features. Research results indicate that early to middle Pleistocene faults in Shandong have a certain controlling effect on earthquakes $M \approx 5.5$.

Neotectonic movements in the region are marked by extensive, sporadic, and uneven patterns of uplift and subsidence, accompanied by significant differential block movements in localized areas. The terrestrial geomorphology is predominantly shaped by North China Plain and the central Shandong mountains, with limited coastal zones in the northeastern and southeastern regions, particularly around Bohai and Southern Yellow Seas. The area also contains various basins, such as Eastern North China Basin, fault depression basins along Yihe River-Shuhe River fault zone, and basins within West Shandong Block, each exhibiting unique developmental histories, classifications, and varying influences from fault activity. The contemporary tectonic stress field in the region is primarily aligned east-northeast to west-southwest for compressional forces, with tension forces oriented nearly north-south. This stress regime is predominantly horizontal or near-horizontal, with an action angle generally below 30°. The overall characteristics of the stress field are largely in line with the broader North China regional stress field. Examination of the combination of the two nodal planes with P and T axes indicates a high probability of right-lateral strike-slip on northeast-oriented faults and left-lateral strike-slip on northwest-oriented faults. The region mainly encompasses North China Plain Seismic Statistical Area and Tancheng-Lujiang Seismic Statistical Area. The engineering site falls within North China Plain Seismic Statistical Area, where the seismic activity level over the next century should not be assumed to be lower than the long-term average. Tancheng-Lujiang Seismic Statistical Area should anticipate the average activity level during its active periods over the next hundred years. Presently, the region is in the fourth active period of North China, and conservatively, there remains a possibility of earthquakes of $M \approx 7.0$ occurring within the next century. A comprehensive analysis indicates that the region possesses the structural prerequisites to undergo earthquakes $8.5 \geq M \geq 6.0$.

Discussion and conclusion

This study provides a systematic analysis of seismic activity in the Shandong region, focusing on its seismicity, major fault structures, spatiotemporal distribution, and associated earthquake hazards. To enhance the robustness and applicability of our conclusions, it is essential to place these findings within a broader global seismological context.

The tectonic evolution of the Shandong region is largely shaped by the interactions among the Eurasian, Philippine Sea, and Pacific plates, making it a typical example of a triple junction zone. The sutures between these plates, along with subduction, collision, and transform faulting, contribute to the formation of the regional fault systems and stress accumulation mechanisms. This dynamic is similar to that observed in other triple junction regions, such as the Gokova Gulf in the Mediterranean. The Gokova Gulf is characterized by significant seismic clustering, with seismic activity displaying spatial heterogeneity and banded aggregation, akin to patterns seen in the Shandong region[56]. Research, such as that by Toker et al. (2023)[53], highlights that triple junctions often experience complex and variable stress-release patterns, with large earthquakes sometimes occurring nearly simultaneously or in rapid succession. Changes in plate interaction rates, such as accelerated subduction or increased strike-slip activity, can trigger or amplify seismic events along multiple fault lines, leading to clusters of large earthquakes. This phenomenon is evident in Shandong, where large earthquakes tend to concentrate along the main segments of the Tanlu Fault Zone and its associated branches, particularly in regions like the Jiaodong Peninsula.

The seismic activity in these regions is driven by collective stress adjustments across multiple plate boundaries and fault systems. In Shandong, similar deformation characteristics are observed along the Tanlu Fault and Jiaolai Basin Fault, where large earthquakes in one segment can significantly affect neighboring fault segments due to stress redistribution. This highlights the importance of monitoring fault zones in close proximity to each other to better understand potential interactions and cascading seismic events.

Building upon these observations, future research should integrate insights from other triple junctions to explore the interactions between faults of varying orientations and the potential for large earthquakes to occur in rapid succession. Such studies will help refine the assessment of triggering mechanisms and improve the understanding of the spatial distribution of seismic events in the Shandong region.

Moreover, major earthquakes often exhibit temporal clustering and spatial migration. The Shandong region, with significant historical events such as the M8½ Tancheng-Dayinzhuang Earthquake in 1668, presents an opportunity to investigate whether similar clustering or migration patterns exist in this area. Further research, incorporating fault geometry studies, stress-field numerical modeling, and strain measurement data, is essential to verify these patterns and enhance our predictive capabilities for future seismic events.

This study provides a systematic analysis of seismic activity characteristics, major fault structures, and the potential hazards associated with the spatiotemporal distribution of seismic parameters in the Shandong region, yielding the following new insights and conclusions:

The findings indicate that moderate to strong earthquakes (especially those of magnitude 6 and above) in the Shandong region mainly occur in belt-like patterns along known active fault zones, particularly exemplified by the Tanlu Fault and the Jiaolai Basin Fault. Although prior research has highlighted fault controls on seismicity, this study refines the segmentation characteristics and hypocenter depth distributions of these fault zones by integrating historical seismic catalogs and precise relocations of modern microearthquakes. By combining historical destructive earthquake data with modern microseismic observations, we confirm that earthquake activity in Shandong is primarily concentrated in the middle to upper crust (approximately 15–20 km depth). This depth distribution aligns with the strike-slip characteristics of the Tanlu Fault Zone. Similar to other triple-junction areas, the frequent recurrence and spatial clustering of shallow-focus earthquakes underscore the heightened importance of earthquake preparedness and disaster mitigation in this region.

Due to the convergence of the Eurasian, Philippine Sea, and Pacific plates, crustal deformation in Shandong is governed not only by individual fault activities but also by collective stress adjustments among multiple faults and tectonic blocks. Drawing on recent findings in regions such as Anatolia[53,56], a significant earthquake on one major fault segment could redistribute stress, affecting adjacent segments and potentially prompting clustered large earthquakes or spatial migration of seismic activity[57–59]. This mechanism explains the historical clustering of major earthquakes in Shandong and highlights the need for integrated assessments of primary and subsidiary faults. Given that Shandong is currently in the fourth active seismic period for North China-coupled with historical evidence, such as the M8½ Tancheng-Dayinzhuang Earthquake in 1668-it is prudent to anticipate the possibility of magnitude 7 or larger events over the next century[60,61]. This study's integrated analysis of seismicity, triple-junction plate dynamics, and fault geometry indicates that strong earthquakes (magnitude 7 or even 8^{+}) may still occur in the region. Lessons from other triple-junction areas show that changes in plate interactions (e.g., accelerated subduction, increased strike-slip rates) could activate multiple faults nearly simultaneously. Hence, urban planning and engineering design near major fault zones must adopt stronger seismic fortification requirements, with particular attention to detailed site investigations and continuous monitoring in fault-prone areas.

While constructing a refined picture of seismic activity in Shandong, this study did not have access to the full range of station azimuths and gaps data, potentially affecting the accuracy of deep structural interpretations, detailed fault segmentation, and focal mechanism solutions. Future work will seek to collect additional observational and mapping data, incorporate high-precision strain measurements, conduct stress-field numerical modeling, and refine fault geometry assessments. These efforts will advance our understanding of multi-fault interactions, potential mainshock-triggering modes, and patterns of large earthquake migration in Shandong, ultimately providing more reliable scientific support for regional seismic risk assessment and disaster mitigation strategies.

In summary, by drawing parallels with other highly seismically active triple-junction regions, this study deepens our understanding of the Shandong region's fault structures, seismicity distribution, and potential triggering mechanisms. The findings contribute valuable insights and parameters for subsequent seismic hazard evaluations and disaster-preparedness efforts in the region. Building on these results, we propose several future research directions to further enhance our understanding of seismic activity in Shandong and improve earthquake disaster prevention and mitigation capabilities. Firstly, it is recommended to investigate the relationship between seismic activity and deep geophysical fields, such as crustal structure and lithospheric rheological properties, to explore the control mechanisms of deep geological processes on shallow seismic activity. Secondly, research should focus on optimizing seismic monitoring networks and earthquake early warning technologies to improve real-time monitoring and rapid response capabilities, thereby reducing the impact of earthquake disasters. Additionally, further improvement of seismic hazard assessment models is necessary by incorporating more factors that influence seismic activity, such as climate change and human engineering activities, to enhance the accuracy and reliability of assessment results. Through these targeted research efforts, more scientific and comprehensive support will be provided for seismic risk management and disaster mitigation strategies in the Shandong region.

Data availability

The datasets generated during and analyzed during the current study are available from the corresponding author on reasonable request.

Received: 10 August 2024; Accepted: 27 March 2025
Published online: 10 April 2025

References

1. Yin, H. et al. Analysis of prensent movement state of Shandong surrounding block. *J. Geodesy Geodyn.* **31**, 37–40 (2011).
2. Li, J., Chen, H. & Wang, Y. Disaster simulation under the scenario of historical Tancheng earthquake in Shandong Province (II) redistribution of disaster relief materials and disaster preparedness strategy. *J. Nat. Disasters* **23**, 75–80 (2014).
3. Xiong, Z. et al. Preliminary discussion on the possible area of strong earthquake occurrence in future along the Shandong-Jiangsu-Anhui segment of Tancheng-Lujiang fault zone. *Seismol. Geol.* **38**, 964–977 (2016).
4. Sawires., R., Santoyo., M. A. & Pelaez., J. A. Corona Fernandez. An updated and unified earthquake catalog from 1787 to 2018 for seismic hazard assessment studies in Mexico. *Sci. Data* **06**, 241. https://doi.org/10.1038/s41597-019-0234-z (2019).
5. Rollins, C. et al. The magnitude-frequency distributions of earthquakes in Aotearoa new Zealand and on adjoining subduction zones, using a new integrated earthquake catalog. *Bull. Seismol. Soc. Am.* **01**, 150–181. https://doi.org/10.1785/0120230177 (2024).
6. Rotondi, R. & Garavaglia, E. Statistical analysis of the completeness of a seismic catalogue. *Nat. Hazards* **25**, 245–258. https://doi.org/10.1023/A:1014855822358 (2002).
7. Chen, Y. et al. A method for simulating rock with inherent microcracks and calibrate its microscopic parameters. *Rock. Mech. Rock. Eng.* https://doi.org/10.1007/s00603-025-04422-x (2025).
8. Liu, Z. et al. Centrifuge model tests and numerical simulation on ground-borne vibration propagating and vibration reduction scheme for tunnel inner structure. *Tunn. Undergr. Space Technol. Incorporat. Trenchl. Technol. Res.* **153**, 105996 (2024).
9. Liu, Z. et al. The geological origins and soil properties of loess-like silty clay: a case study in the Jinan area. *Sci. Rep.* **14**, 12612 (2024).
10. Ma, X. et al. Characteristics of physical parameters and predictive modeling of mechanical properties in loess-like silty clay for engineering geology. *Eng. Geol.* **339**, 1–15 (2024).
11. Liu, Z. et al. DNN–GA–RF prediction model for rock strength indicators based on sound level and drilling parameters. *Bull. Eng. Geol. Environ.* **83** (9), 360 (2024).
12. Zhang, Z. et al. Scaled model tests on pile types influencing the stability of stiffened deep mixed pile-supported embankment over soft clay. *Acta Geotech.* https://doi.org/10.1007/s11440-024-02424-7 (2024).
13. Nurminen, F. et al. SURE 2.0-New release of the worldwide database of surface ruptures for fault displacement hazard analyses. *Sci. Data* **09**, 729. https://doi.org/10.1038/s41597-022-01835-z (2022).

14. Department of Earthquake Disaster Prevention, China Seismological Bureau. Catalog of historical Strong Earthquakes in China (23rd century B.C. to 1911). (1995).
15. Department of Earthquake Disaster Prevention, China Seismological Bureau. The Catalog of Modern Earthquakes in China, 1912 ~ 1999, Ms ≥ 4.7. (1999).
16. Department of Earthquake Disaster Prevention, China Seismological Bureau. The Catalog of Modern Earthquakes in China, 1912 ~ 1999, Ms ≥ 4¾. (1999).
17. Department of Monitoring and Forecasting, China Seismological Bureau. Compilation of the Catalogue of Earthquakes of magnitude 5 or higher in China (1900–2022). (2023).
18. Ji, A., Zhou, Y. & &Li, B. Monitoring capacity of Shandong digital seismic network. *J. Seismol. Res.* **02**, 132–136 (2009).
19. Gao, R. & &Xie, J. Discussion on the minimum magnitude of completeness in the earthquake catalogue in the Henan area. *Seismol. Geomag. Observ. Res.* **05**, 21–25. (2021).
20. Li, X., Zhang, X. & &Hu, B. Monitoring capacity of the digital telemetric seismic network of Hebei Province. *Earthq. Res. Shanxi* **02**, 22–2443 (2005).
21. Shi, Z. Earthquake work manual. (1990).
22. Shandong Provincial Earthquake Historical Data Editing Office. Compilation of earthquake historical materials in Shandong Province. (1983).
23. Shandong Provincial Earthquake Bureau. Earthquake Catalogue of Shandong Province (1968–1980). (1986).
24. Shandong Provincial Earthquake Bureau. Earthquake Catalogue of Shandong Province (1981–1990). (1995).
25. Shandong Provincial Earthquake Bureau. Earthquake Catalogue of Shandong Province (1991–2007). (2010).
26. Wei, G. et al. Investigation of modern felt earthquakes in Shandong (1968–1992). (1998).
27. Ma, Z. et al. Nine major earthquakes in China from 1966 to 1976. (1982).
28. Wang, H. Holocene displacement rate, Paleo earthquakes and recurrence intervals of strong earthquakes along the 1668 Tancheng earthquake (Ms = 8.5) fault. *China Earthq. Eng. J.* **04**, 1–12 (1995).
29. Wang, X. The deep tectonic studies of Yishu fault zone. *Earthq. Res. China* **03**, 29–35 (1988).
30. Chao, H. et al. Seismic tectonic map of Shandong Province, new tectonic map and description of Shandong Province (1:1 million). (1997).
31. Wei, G. et al. Studies of seismic activity in Tanlu fault. (1993).
32. Du, Y. The main latent fault study in Jinan. (2005).
33. Chao, H. et al. The N-W trending faults in middle part of Shandong province and their activities in the late quaternary. *J. Disaster Prev. Mitigation Eng.* **02**, 1–10 (1992).
34. Gao, W. et al. An overview of the research results of seismic risk assessment and intensity zoning in Southern Shandong. *Earthq. Res. China* **03**, 7–9 (1988).
35. Wang, H. et al. Earthquake Research and Seismic Zoning in Qingzhou, Shandong. (1995).
36. Xiang, H. et al. Integrated survey and investigation on the quaternary activity of the Liaocheng-Lankao buried fault. *Seismol. Geol.* **04**, 351–359 (2000).
37. Han, Z. et al. Active blocks and strong seismic activity in North China region. *Sci. China Ser. Earth Sci.* **46**, 153–167. https://doi.org/10.1360/03dz0012 (2004).
38. Li, C. &Wang,Z. Tectonic division of the upper crust of the North China block. *Earth Sci. Front.* **16**, 215–224 (2009).
39. Koji, U. & Huang, B. Constraints on the jurassic swing of the apparent polar wander path for the North China block. *Geophys. J. Int.* **154**, 801–810. (2009).
40. Jia, S. & Zhang, X. Crustal structure and comparison of different tectonic blocks in North China. *Chin. J. Geophys.* **48**, 672–683 (2005).
41. Xi, X., Andrew, V. & Lin, C. Late cretaceous to early cenozoic extension in the lower Yangtze region (East China) driven by Izanagi-Pacific plate subduction. *Earth Sci. Rev.* **221**, 103790. https://doi.org/10.1016/j.earscirev.2021.103790 (2021).
42. Wang, W. et al. Spatial and temporal evolution of Ediacaran carbon and sulfur cycles in the Lower Yangtze Block, South China. *Palaeogeogr. Palaeoclimatol. Palaeoecol.* **537**,109417. https://doi.org/10.1016/j.palaeo.2019.109417 (2020).
43. Chen, M., Zheng, J., Sun, M. & Zhao, J. Mid-Neoproterozoic crustal evolution of the Northeastern Yangtze block: evidence from the felsic-gneiss xenoliths hosted in the Donghai cenozoic basalts. *J. Asian Earth Sci.* **66**, 108–122. https://doi.org/10.1016/j.jseaes.2012.12.032 (2013).
44. Ye, Z. et al. A seismic receiver function study for the crustal and upper mantle structures of the lower Yangtze and adjacent areas and its geological implications. *Acta Geol. Sin.* **94** (3), 707–715. https://doi.org/10.19762/j.cnki.dizhixuebao.2020153 (2020).
45. Chao, H. et al. The latest activities of faults in the Taian region, Shandong Province and the Taishan mountain earthquake. *Seismol. Geol.* **02**, 10–19 (1999).
46. Wang, J. & Main, I. G. Strong historical earthquakes and their relationships with the Tan-Lu fault system and modern seismicity in Eastern China. *Nat. Hazards* **115**, 539–564. https://doi.org/10.1007/s11069-022-05565-8 (2023).
47. Pang, C. et al. Sequence of earthquake episodes and occurrences in a neoproterozoic seismically active phase in Southern Shandong, China. *Geol. Bull. China* **26** (9), 1198–1205. https://api.semanticscholar.org/CorpusID:130665479 (2007).
48. Li, X. et al. Relocation of earthquakes in Shandong and its neighboring areas. *China Relatsh. Act. Tectonics* **28** (4), 381–392 (2013).
49. Du, G. et al. Research on neotectonic differentiation of geo-information in Shandong Peninsula. *Geotectonica Metallogenia* **30**, 114–119 (2006).
50. Wan, Y. et al. Contemporary tectonic stress field in China. *Earthq. Sci.* **04**, 377–386 (2000).
51. Dong, X. et al. Study on tectonic stress field and the seismicity in Shandong area. *Plateau Earthq. Res.* **03**, 37–43 (1999).
52. Zhou, C. et al. Analysis on recent stress background in Shandong Province. *Earthq. Res.* **04**, 54–61 (1992).
53. Toker, M., Yavuz, E., Utkucu, M. & Uzunca, F. Multiple segmentation and seismogenic evolution of the 6th February 2023 (Mw 7.8 and 7.7) consecutive earthquake ruptures and aftershock deformation in the Maras triple junction region of SE-Anatolia, Turkey. *Phys. Earth Planet Inter.* **345**, 107–114. https://doi.org/10.1016/j.pepi.2023.107114 (2023).
54. Toker, M., Pınar, A. & Hoskan, N. An integrated critical approach to off-fault strike-slip motion triggered by the 2011 Van mainshock (Mw 7.1), Eastern Anatolia (Turkey): New stress field constraints on subcrustal deformation. *J. Geodyn.* **147** (101861), 1–25. https://doi.org/10.1016/j.jog.2021.101861.((2021).
55. Irmak, T. S., Toker, M., Yavuz, E., Şentürk, E. & Güvenaltın, M. A. New insight into the 24 January 2020, Mw 6.8 Elazığ earthquake (Turkey): An evidence for rupture-parallel pull-apart basin activation along the East Anatolian Fault Zone constrained by Geodetic and Seismological data. *Ann. Geophys.* 64. https://doi.org/10.4401/ag-8638 (2021).
56. Toker, M. Symptomatic discretization of small earthquake clusters reveals seismic coupling to 2017 Bodrum earthquake (Mw 6.6) in the Gulf of Gökova (SW corner of Turkey): Viscous-compliant seismogenesis over back-arc setting. *J. Afr. Earth Sci.* **177** (104156). https://doi.org/10.1016/j.jafrearsci.2021.104156.((2021).
57. Zhou, C. et al. Recent tectonic stress field and seismicity in Yihe-Shuhe fault belt. *North China Earthq. Sci.* **02**, 29–39 (1987).
58. Huang, W. et al. Research on the completeness of earthquake data in the Chinese mainland (I) - North China. *Acta Seismol. Sin.* **03**, 273–280 (1994).
59. Huang, W. et al. Research on completeness of earthquake data in the Chinese mainland (II) -The regional distribution of the beginning years of basically complete earthquake data. *Acta Seismol. Sin.* **04**, 423–432 (1994).
60. Jiao, Y. et al. Detectability of seismic network in North China. *Earthquake* **01**, 26–32 (1986).

61. Wang, L., Mao, G., Wang, H. & Mu, L. Digital method and preliminary study of Hebei historical simulated seismograms. *J. Geodesy Geodyn.* **43**, 703–707 (2023).

Acknowledgements
This work was supported by the Key R&D Program of Shandong Province (2021CXGC011203) and the China Scholarship Council (NO.202406260135) in China.

Author contributions
Linhai Lu: survey management, data acquisition, processing, and validation. Zhenghao Liu: project conception, writing - original draft, writing - review and editing. Hanwen Zhang: writing - review and editing. Chaojun Wu: data acquisition, processing, and validation. Jiecheng Sun: data acquisition, processing, and validation. Xianfeng Ma: Survey management, data acquisition. Dingyi Zhou: data acquisition, processing, and validation. Han han: writing - review and editing. Haojin Zhang: writing - review and editing. Rui Li: writing - review and editing.

Declarations

Competing interests
The authors declare no competing interests.

Additional information
Supplementary Information The online version contains supplementary material available at https://doi.org/10.1038/s41598-025-96305-y.

Correspondence and requests for materials should be addressed to Z.L. or X.M.

Reprints and permissions information is available at www.nature.com/reprints.

Publisher's note Springer Nature remains neutral with regard to jurisdictional claims in published maps and institutional affiliations.

Open Access This article is licensed under a Creative Commons Attribution-NonCommercial-NoDerivatives 4.0 International License, which permits any non-commercial use, sharing, distribution and reproduction in any medium or format, as long as you give appropriate credit to the original author(s) and the source, provide a link to the Creative Commons licence, and indicate if you modified the licensed material. You do not have permission under this licence to share adapted material derived from this article or parts of it. The images or other third party material in this article are included in the article's Creative Commons licence, unless indicated otherwise in a credit line to the material. If material is not included in the article's Creative Commons licence and your intended use is not permitted by statutory regulation or exceeds the permitted use, you will need to obtain permission directly from the copyright holder. To view a copy of this licence, visit http://creativecommons.org/licenses/by-nc-nd/4.0/.

© The Author(s) 2025